Localized triplet excitations and the effect of photo-oxidation in ladder-type poly(*p*-phenylene) and oligo(*p*-phenylene)

E. J. W. List
Institut für Festkörperphysik, Technische Universität Graz, A-8010 Graz, Austria
and Ames Laboratory-United States Department of Energy and Department of Physics and Astronomy, Iowa State University, Ames, Iowa 50011

J. Partee and J. Shinar
Ames Laboratory-United States Department of Energy and Department of Physics and Astronomy, Iowa State University, Ames, Iowa 50011

U. Scherf and K. Müllen
Max-Planck-Institut für Polymerforschung, Mainz, Germany

E. Zojer, K. Petritsch, and G. Leising
Institut für Festkörperphysik, Technische Universität Graz, A-8010 Graz, Austria

W. Graupner
Department of Physics, Virginia Tech, Blacksburg, Virginia 24060

(Received 22 December 1998; revised manuscript received 27 August 1999)

The photophysics of methyl-bridged poly(para-phenylene)-type ladder polymer (m-LPPP) and oligomer films and solutions is described and discussed. The spin sensitive properties, such as the formation and properties of polaron pairs and triplet excitons (TE's) were studied using *X*-band photoluminescence (PL) detected magnetic resonance (PLDMR). The PLDMR results and quantum chemical calculations show unambiguously that the TE wave-function extent is much smaller than that of the singlet exciton (SE). The weaker vibronic structure of the triplet photoinduced absorption (PA) band of m-LPPP relative to the singlet absorption is assigned to the small energy difference between the geometry of the lowest lying and excited triplet states. This is an additional indication of the strong localization of the triplet wave-function as compared to that of the SE. Finally, the influence of photo-oxidation on the PLDMR and PA is analyzed and discussed in relation to the photoconductivity of the materials.

I. INTRODUCTION

The class of poly(*p*-phenylene)-type ladder-polymers (LPPP's) is highly attractive for applications in organic light-emitting diodes[1] (OLED's) due to its high photoluminescence (PL) quantum yield of ~30% in film and ~100% in solution.[2] The interring bridges that are added to poly(para-phenylene) (PPP) result in a planarization of neighboring phenyl rings, which increases the π conjugation and therefore leads to a redshift of the electronic optical spectra. Due to the sidegroups attached to the backbone, excellent solubility is achieved in common organic solvents such as chloroform and toluene, a prerequisite for the preparation of high-optical quality films. The high degree of intrachain order[3,4] and the well-defined conjugation length of methyl-substituted ladder-type PPP (m-LPPP) (see Fig. 1) are the reason for its potential use as the active medium in organic solid-state lasers.[5] A wide spectral range of emission colors, including white light,[6] can be accomplished using a polymer-doped active m-LPPP layer.[7] In addition, due to its well-resolved spectroscopic features in absorption and emission this material has been studied extensively as a model system with various cw (Ref. 8) and time resolved spectroscopic techniques.[9]

Simple spin-statistical considerations predict that 25% of the recombining nongeminate polaron pairs generated by carrier injection in an OLED will yield singlet excitons (SE's) whereas the other 75% will yield nonradiative triplet excitons (TE's), which theoretically limits the quantum yield of the OLED to 25%. However, it was suggested that the

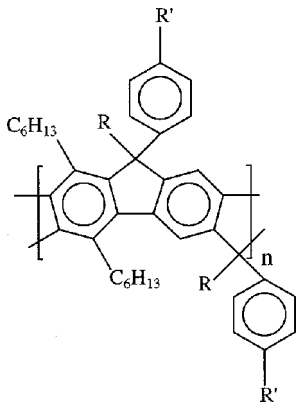

FIG. 1. Chemical structure: For m-LPPP R=CH_3, R′ =$C_{10}H_{21}$, $n \approx 25$. For LOPP7 R=H, R′=CH_3 with the backbone consisting of 7 phenyl rings.

strong difference in the nature of the SE and TE states influences the formation cross-section of SE's and TE's from polarons.[10,11] Therefore it is highly desirable to investigate the nature of TE's and their spin-dependent formation from polaron pairs as well as from SE's.

This paper explores the spatial extent of the triplet wave functions through the spin dependent photophysical properties of m-LPPP and the seven-membered ladder-type oligo(*p*-phenylene) (LOPP7) as monitored by their *X*-band photoluminescence (PL)-detected magnetic resonance (PLDMR) spectra. In π-conjugated molecules TE's are known to be highly localized with a spatial extent of $\sim$0.3 nm while SE's are much more delocalized with a typical extent of $\sim$2 nm.[12]

The PLDMR spectra of π-conjugated polymers such as poly(3-alkyl thiophenes) (P3AT's),[13] poly(*p*-phenylene vinylenes) (PPV's),[14] and poly(*p*-phenylene ethynylenes) (PPE's) (Ref. 15) typically exhibit three PL-enhancing features when excited at $\lambda_{exc} \geqslant 458$ nm:

(i) a 5–80 G-wide so-called polaron pair resonance at $g = 2.0023 \pm 0.001$, which monitors the influence of the magnetic resonance-enhanced recombination of relatively distant polaron pairs[16,17] on the PL;

(ii) a 500–1200 G-wide full-field triplet powder pattern and

(iii) the 20–35 G-wide half-field triplet powder pattern; (ii) and (iii) reveal information on the localization of the TE's as well as on their interaction with SE's.

In the present work the formation yield of polarons is also studied by (i) comparing the polaron pair resonance of pristine and photo-oxidized m-LPPP films and (ii) monitoring the polaronic absorption observed in photoinduced absorption (PA). The results are discussed in relation to the photocurrent of devices fabricated from m-LPPP. Finally, the effect of the localization of the TE's on the vibronic modes in the triplet PA band is also discussed.

II. EXPERIMENTAL PROCEDURE

The synthesis of m-LPPP and of the LOPP's was described elsewhere.[18,19]

Samples for PLDMR measurements were prepared by dissolving the polymer or oligomer powder in toluene in a 4-mm OD quartz tube. The toluene was then evaporated leaving a $\sim$200 nm-thick film on the inside walls of the tube. Solution samples were prepared by freezing the 3 mg/ml toluene solution in the quartz tube, degassing it, and vacuum sealing the tube. To study the effects of photo-oxidation the samples were exposed to air and the light of a 200 W xenon lamp for $\sim$30 min.

The sealed sample tubes were placed in the quartz dewar of an Oxford Instruments He gas-flow cryostat, enabling temperature control from 4–300 K, inside an optically accessible 9.35 GHz *X*-band microwave cavity. The PL was excited at 457.9 nm by a Pockels-cell stabilized Ar^+ laser. The excitation power was kept at or below 30 milliwatts to prevent sample heating. The PL and PLDMR spectra were measured using a Si photodiode; the laser line was blocked by an appropriate cutoff filter. The changes in the PL intensity induced by the *X*-band microwaves at the applied dc magnetic field were detected by feeding the photodiode output into a lock-in amplifier referenced by the microwave chopping frequency $400 \leqslant \nu_c \leqslant 900$ Hz. The microwave power was kept below 810 mW.

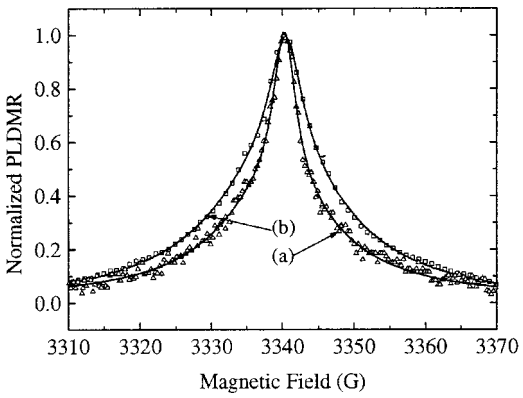

FIG. 2. Polaron resonance of (a) a pristine m-LPPP film and (b) after 30 min. photo-oxidation. The lines represent the double Lorentzian fits. $\lambda_{exc} = 457.9$ nm, laser power 20 mW, $T = 20$ K, and microwave power 40 mW.

Samples for PA measurements were prepared by spin coating Infrasil substrates from a toluene solution of m-LPPP. The pump beam was produced by an Ar^+ laser with a laser power of approximately 240 mW, which was mechanically chopped at $\sim$89 Hz, providing the reference for the lock-in amplifier. The sample was mounted in an optically accessible cryostat under a dynamic vacuum of less than 10^{-5} mbar. A 50 W tungsten halogen lamp was the light source for the transmission measurement. All PA spectra were measured at 90 K and were corrected for PL and the optical throughput of the setup.

III. RESULTS AND DISCUSSION

A. Effect of photo-oxidation of m-LPPP

Photo-oxidation was previously found to be a major irreversible PL-quenching mechanism in π-conjugated polymers such as PPV. It was found that the SE emission is strongly quenched by carbonyl groups, which the IR spectra of the photo-oxidized films revealed.[20] It is known that illuminating m-LPPP films with a 200 W Xenon lamp in air for 30 mins breaks the group stabilizing the planarity of the backbone and consequently destroys its extraordinary high intrachain order.[21] In this section, we compare the polaron pair resonance and PA spectra of pristine and photo-oxidized m-LPPP films and discuss the observed results in relation with the photocurrent of devices fabricated from m-LPPP to gain insight into the processes resulting from photo-oxidation.

1. The polaron pair resonance

Figure 2 shows the normalized polaron resonance spectra of (a) a pristine and (b) a photo-oxidized m-LPPP film at 20 K excited at $\lambda_{exc} = 457.9$ nm. Due to the irreversible loss of the intrachain order and the drastic increase in the number of PL quenching sites the PL intensity decreased dramatically to 15% of the pristine film's value. However, at the same time the polaron PLDMR amplitude $\Delta I_{PL}/I_{PL}$ increased by a factor of 4.

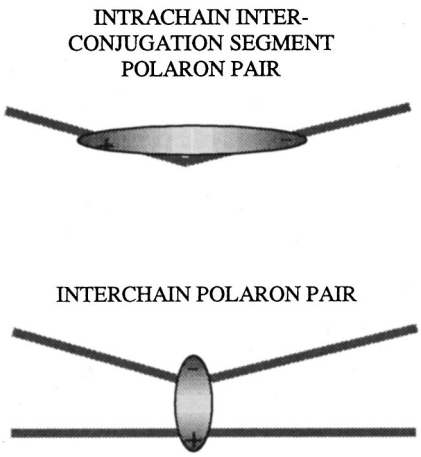

FIG. 3. Schematics of intrachain interconjugation-segment polaron pairs and interchain polaron pairs.

Each of the polaron pair resonances was fitted to the sum of a broad low-field and a narrow high-field Lorentzian, since the double Lorentzians provided better agreement with the observed lineshape than double Gaussians. Upon photo-oxidation, the linewidths of the low- and high-field components increase from 21.0 and 3.7 G to 26.1 and 5.0 G, respectively. The ratio of the integrals of the broad-to-narrow Lorentzian increases from 3.8 to 6.6. One also finds that in all fits the center fields of the two Lorentzians were separated by 1.0–1.5 G, corresponding to a difference of 0.00065–0.001 in the g factors, with the narrower component always having the lower g value.

The observed higher and lower g-values (lower and higher fields, respectively) of the broad and a narrow Lorentzians, respectively, are similar to the resonance positions in P3AT films and solutions.[12,22] An interpretation of this observation, however, is difficult since the absolute positions of the peaks cannot be determined sufficiently accurately. As discussed in detail below, due to a difference in the polaron pair distance, the polaron pairs are subject to slightly different local fields, which leads to slightly different g factors.

The fit to two Lorentzians is related to the assumption of different average separations of two types of polaron pairs as depicted in Fig. 3. The narrower component is assigned to more distant pairs, mainly intrachain-interconjugation-segment pairs. Such pairs form on the same chain between different conjugation segments, e.g., due to a broken interring bridge in the polymer backbone, which is a stabilizing defect. The broader component is assigned to closer polaron pairs, mainly interchain.[23] Such pairs form if, e.g., a SE dissociates by a charge transfer process of the electron onto a neighboring chain. The charge transfer process can be initiated by the presence of an electrophilic defect such as a carbonyl group on the neighboring chain.

The finding of an overall increased $\Delta I_{PL}/I_{PL}$ as well as the observed broadening of the resonance line upon photo-oxidation is therefore attributed to a higher overall steady-state density of interchain polaron pairs due to the fact that upon photo-oxidation one increases the density of carbonyl groups[20] acting as charge transfer centers dissociating SE's. We note that such interchain pairs can moreover dissociate into free polarons and/or recombine to TE's as observed in PA. (see also next Section).

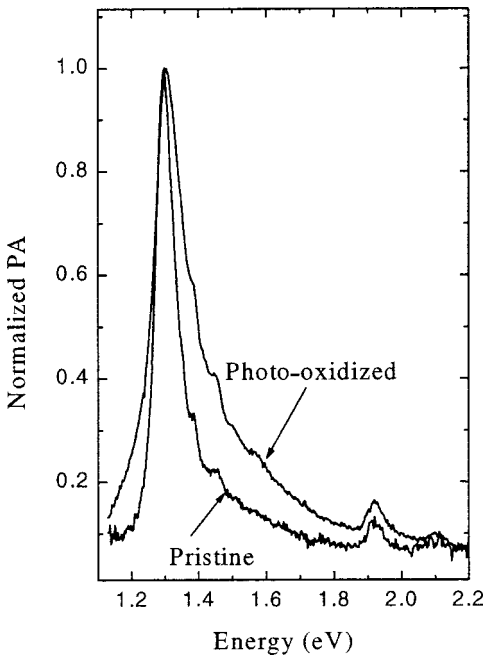

FIG. 4. PA spectrum of (a) a pristine m-LPPP film and (b) after 30 min. photo-oxidation. $\lambda_{exc}=457.9$ nm and $T=20$ K .

2. The photoinduced absorption of m-LPPP

Figure 4 shows the PA spectrum of pristine and photo-oxidized m-LPPP films. By comparing the PA spectrum with doping- and charge-induced absorption spectra, where only the 1.9 eV band is observed,[24] the PA bands at 1.3 and 1.9 eV were assigned to triplet-to-triplet ($T_1 \rightarrow T_n$) and trapped polaron transitions, respectively. Upon photo-oxidation the integrated intensity of these bands increases by 100% and the full width at half maximum of the $T_1 \rightarrow T_n$ band increases from 70 meV to 137 meV. In addition, a small blue-shift of the $T_1 \rightarrow T_n$ transition occurs, while the energies of the polaron bands do not change within experimental resolution.

The controlled change in the polymer achieved by photo-oxidation, which broadens and slightly blue-shifts the $T_1 \rightarrow T_n$ PA band, indicates a loss of intrachain order, i.e., a reduction in the effective conjugation length. The growth of the polaron PA band intensity demonstrates that carbonyl groups dissociates SE's, thus acting as charge transfer centers. Moreover these defects also stabilize the polarons, i.e., increase their lifetime, which in turn increases their steady-state density.

The striking fact that the observed triplet steady state density increases by the same magnitude as observed for polaronic absorption can be attributed to two different effects: (a) an increased formation of TE's formed by the recombination of polarons due to the higher polaron population or (b) an increased intersystem crossing rate as a consequence of the presence of carbonyl groups.

As reported previously photo-oxidation of m-LPPP in single-layer solar cells enhances the observed photocurrent by an order of magnitude.[25] In the absence of a dark current the observed photocurrent is proportional to the mobility and the photogenerated carrier density. Since the increase of the number of trap-sites upon photo-oxidation does not increase carrier mobility, the increase of the photocurrent has to be assigned to the higher formation rate of interchain polaron

pairs, which is again due to oxygen defect-induced dissociation of SE's into free polarons. This in summary shows that the degradation of the material strongly enhances the generation of polarons from SE's, which is also fully consistent with the absence of an IR polaron band in PA (Ref. 26) and the absence of a PL-detected magnetic field effect in pristine m-LPPP,[20] as both originate from defect stabilized polaron pairs.

B. The triplet powder pattern

The full-field triplet powder pattern located at higher and lower magnetic field values with respect to the polaron pair resonance is attributed to the magnetic resonance-enhanced decay of TE's. This may be due either to enhanced triplet-triplet annihilation to SE's, or to a decreased rate of singlet-quenching by triplets.

The observation of a triplet powder-pattern is due to the anisotropic electron-electron spin-interaction, which is given by the spin Hamiltonian H_{ss}:[27]

$$H_{ss}=J_0\mathbf{S}_1\cdot\mathbf{S}_2+D\left(S_{1z}S_{2z}-\frac{1}{3}\mathbf{S}_1\cdot\mathbf{S}_2\right)+E(S_{1x}S_{2x}-S_{1y}S_{2y})+\mathbf{d}\cdot\mathbf{S}_1\mathbf{X}\,\mathbf{S}_2, \quad (1)$$

where J_0 is the exchange term and D and E are the zero field splitting parameters. Within a first approximation $J_0\mathbf{S}_1\cdot\mathbf{S}_2$ can be omitted since it only contributes to the singlet-triplet splitting and does not affect the transitions in the triplet manifold and $\mathbf{d}\cdot\mathbf{S}_1\mathbf{X}\,\mathbf{S}_2$ vanishes within the triplet manifold so that the Hamiltonian only contains the two parameters D and E.[28] Since the Hamiltonians of the exchange and the dipolar interactions are similar one cannot distinguish between them from the triplet powder pattern. The exchange interaction, however, vanishes for distances of more than 3–4 Å between the interacting spins as shown for similar spin systems.[26] However, both interactions yield a full-field powder pattern due to $\Delta m_s=\pm 1$ transitions as well as a half-field pattern due to $\Delta m_s=\pm 2$ transitions.[28]

From the structure of the full-field triplet pattern one can determine D and E. If the interaction of the TE's is predominantly dipolar in nature, i.e., if there is no significant contribution from spin-orbit coupling to D, which is the case for the present class of materials, an estimate for the extent of the triplet wave function r_{ub} is given by

$$r_{ub}\approx C\left(\frac{D}{g\mu_\beta}\right)^{-1/3}(\text{Å}), \quad (2)$$

where $D/g\mu_\beta$ is given in Gauss and $C\approx 24$ (Ref. 12) or $C\approx 30$.[29,30]

The parameter E quantifies the deviation of the triplet wave function from axial symmetry and by definition of D and E, $|E|\leqslant|D|/3$.[27,31–33]. As concluded from other π-conjugated polymers, the x and y axes are assigned to the plane of and the z axis to the normal to the polymer backbone.[34]

1. The full-field triplet powder pattern

The full-field triplet PLDMR powder pattern of pristine and photo-oxidized films and frozen toluene solutions of m-LPPP and LOPP7 are shown in Figs. 5(a)–5(e). The spectra, offset for clarity, all consist of the narrow polaron resonance in the center ($g\approx 2.0$) superimposed on a pattern located at lower and higher magnetic fields. All polaron resonance peaks are cut off due to the high gain of the lock-in amplifier. The m-LPPP film spectrum [Fig. 5(c)] shows a pronounced extended powder pattern. Increasing the temperature from 15 K to room temperature decreases the intensity as well as the extent of the pattern. In the saturated solution of m-LPPP [spectrum (d)] only a weak pattern is observed. Photo-oxidizing the m-LPPP decreased the PL intensity I_{PL} to 15% of the pristine value but increased the triplet PLDMR amplitude $\Delta I_{PL}/I_{PL}$ by 20%. However, except for broadening effects the shape of the pattern did not change.

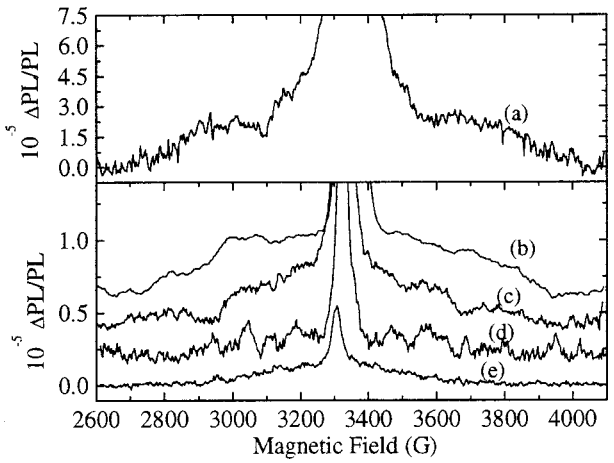

FIG. 5. Full-field powder pattern of (a) a LOPP7 film, (b) a photo-oxidized m-LPPP film at 15 K, (c) a pristine m-LPPP film at 10 K, (d) a saturated frozen m-LPPP solution at 15 K and (e) a m-LPPP film at room temperature. Plots are offset for clarity, $\lambda_{exc}=457.9$ nm, laser power 20 mW, microwave power 810 mW for (a), (c), (d), and (e) and 102 mW for (b).

The powder pattern amplitude of LOPP7 at 15 K is 3–4 times larger than that of a pristine m-LPPP film and the positions of its transitions are altered. In addition, in LOPP7 the pattern weakens below the detection limit at $T>130$ K, in contrast to that of m-LPPP.

The analysis of the full-field pattern of the m-LPPP film yielded $|D/g\mu_\beta|\approx 620$ G and $|E/g\mu_\beta|\approx 6$ G. (see the Appendix). Due to extreme broadening of the lines of the powder pattern of the photo-oxidized m-LPPP, we could only estimate $|D/g\mu_\beta|\approx 620$ G from the total extent of the full-field powder pattern.

The weak triplet resonance of the saturated frozen m-LPPP solutions is not clear at present. The behavior of the room-temperature spectrum is interpreted to be due to averaging of the dipole-dipole interaction.[27] This effect can account for both the decrease of the intensity and width of the powder pattern.

2. The half-field triplet powder pattern

Figure 6 shows the half field resonance of (a) an m-LPPP film, (b) a photo-oxidized m-LPPP film, and (c) an LOPP7 film. We note that $\Delta I_{PL}/I_{PL}$ of the m-LPPP film increased by a factor of 2 upon photo-oxidation. The shape and the

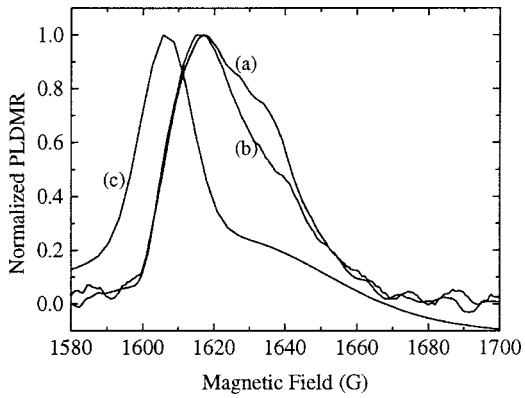

FIG. 6. Half-field powder pattern of (a) a photo-oxided m-LPPP film, of (b) a pristine m-LPPP film and of (c) a LOPP7 film. For all samples $\lambda_{exc}=457.9$ nm, for (a) and (b) microwave power 265 mW, $T=15$ K, laser power 30 mW and for (c) laser power 20 mW, microwave power 810 mW, $T=26$ K (all three plots are smoothed by adjacent averaging).

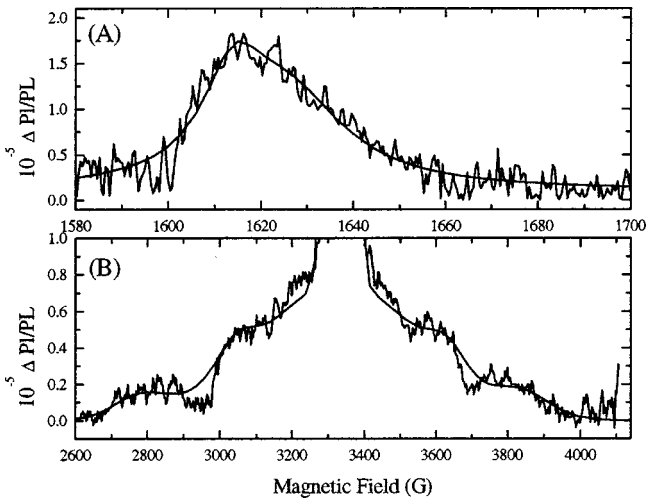

FIG. 7. Simulation of (A) the half-field powder pattern of Figure 6(b) and (B) the full-field powder pattern of Fig. 5(c), with $D=620$ G, $E=6$ G.

magnetic field position are similar with only the shoulder at ~1628 G becoming much more prominent upon photo-oxidation. No half-field powder pattern could be detected at $T>130$ K in these samples.

As shown in Fig. 7 the simulations (see Appendix) for the half-field (A) and full-field (B) spectra of the m-LPPP film are in good agreement with the observed spectra. At $g\approx2.00$ we added a Lorentzian to account for the polaron resonance.

The asymmetry of the powder pattern with respect to $g=2.0023$ is also observed in other polymers such as substituted polythiophene where it is found to be more pronounced.[35] In order to account for this small asymmetry in the simulation one has to consider a difference in the g factors of 0.013 between the central resonance and the powder pattern. Since the central resonance is attributed to the recombination of more distant polaron pairs,[15] which are not coupled via a dipole-dipole or anisotropic exchange interaction, its g-factor is expected to be closer to the free electron g value 2.0023. The increase of the g-factor of the dipolar-broadened polaron pairs with a spatial separation of 3–4 Å (see below) which may be viewed as excitons in their triplet ground state, is caused by a small orbital angular momentum. This contribution is well known to result in an effective change of the g factor.[27]

As expected, both the full- and half-field patterns of the photo-oxidized and pristine m-LPPP yield the same value of D. However, the half-field patterns demonstrate that the shoulder at ~1628 G becomes much more prominent upon photo-oxidation. From the analysis one finds that this transition in the half-field corresponds to transitions at around 3000 G and 3660 G in the full-field, which are also found to be more prominent.

The analysis of the extent of the full-field powder pattern of LOPP7 yielded $|D/g\mu_\beta|\approx705$ G whereas from the half-field pattern one finds $|E/g\mu_\beta|\approx70$ G.

The values of $|D/g\mu_\beta|$ and r_{ub} obtained from the foregoing analysis are summarized in Table I. Note that we cannot determine the sign of D or E, so it is not possible to tell whether the triplet wave function is oblate (disklike, $D>0$) or prolate (cigarlike, $D<0$). Yet in any case the evaluation yielded a rather small $|E|$ suggesting that the wave-function is nearly axially symmetric with respect to the z axis.

The striking observation that the amplitudes of the triplet powder pattern in LOPP7 is 4 times larger than that of pristine m-LPPP should be discussed in relation to the observed aggregation in the oligomer films as described in detail in Ref. 36. From the PL excitation and emission and PLDMR it was found that the electronic properties of the LOPP films are determined by aggregate states, which are favored by the short substituents in the oligomers and which enhance the formation of free polarons generated by dissociation of the delocalized SE's. Hence, it is believed that aggregation enhances the formation of TE's from free polarons. Since the polaron PLDMR in LOPP7 is an order of magnitude weaker than in m-LPPP we conclude that the contribution of free polarons to the polaron-PLDMR is weaker than that of trapped polarons, possibly due to the difference in their lifetimes.

3. The triplet wave-function extent

In Table I we compare the extent of the triplet wave-function r_{ub} determined from PLDMR with those obtained from time-resolved excited-state microwave polarizability measurements[37] and light induced electron spin resonance of different polymers and oligomers.[29] As clearly seen the three independent experimental methods give similar values of 3–4 Å . The wave-function extent in the oligomers increases with increasing (conjugation) length. The increase from 3.39 Å for LOPP7 to 3.52 Å for m-LPPP is therefore in agreement with the results obtained for PPV (Ref. 36) and P3AT.[12] Furthermore the increase is in good agreement with quantum-chemical calculations for isolated molecules of oligo(phenylene-vinylene)s (Ref. 12) and oligo-(thiophene)s.[38]

C. Quantum-chemical calculations

The estimates for the triplet extent obtained from the half- and full-field PLDMR of LOPP7 are now compared to results of quantum-chemical calculations for an isolated mol-

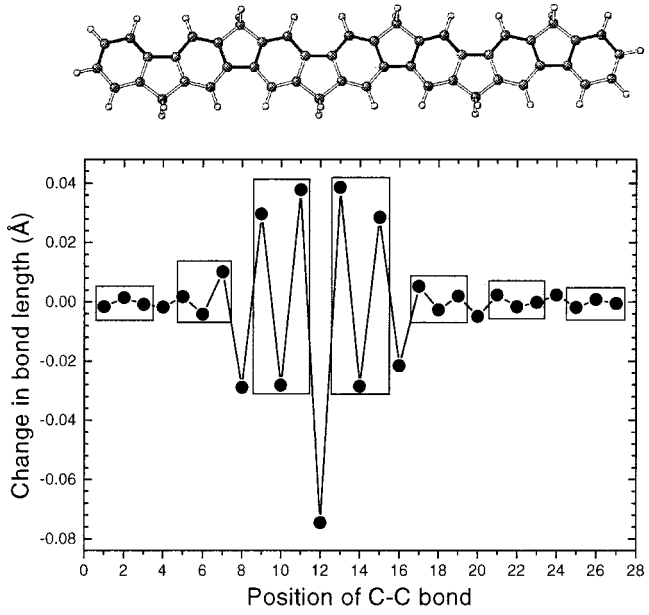

FIG. 8. Bond length modification in the lowest triplet state relative to the singlet ground state calculated for LOPP7 (the sidechains are replaced by methyl units), making use of a semiempirical AM1/MECI approach. The bonds for which the results are shown correspond to the dark lines in the model of the molecule.

ecule containing seven repeat units (see Fig. 8). We estimated the extent of the triplet state from the modifications of the bond lengths associated with the formation of that state. The geometry optimizations used the semiempirical Austin Model #1 (AM1), which is known to provide good estimates for the geometries of organic molecules.[39] For the triplet state the AM1 approach was coupled to a multi electron configuration interaction technique to account for correlation effects with a perturbative algorithm to extract the main electronic configurations contributing to the description of the states of interest.[40] The three highest occupied and the fourteen lowest unoccupied orbitals were active in the configuration interaction calculations. For chains with an odd number of benzene rings like LOPP7 two positions for the TE with similar total energies are possible. One corresponds to a symmetric conformation in which the strongest modifications of the geometry are in the central ring. In the second conformation shown in Fig. 8 the geometry modifications are centered at an interring bond and extend across the two adjacent benzene rings. The energy of the second conformation is calculated to be 9 meV lower than that of the symmetric one, expressing the tendency of the TE to reside on two benzene rings. The resulting strong localization is in good agreement with calculations for oligo(phenylene vinylene)s (Ref. 37) and oligo(thiophene)s.[12]

The spatial extent of the TE is significantly smaller than that of polarons and bipolarons in oligo(phenylenes).[41] The strongest modifications of the TE state occur in the two bonds connecting the central ring to its phenylene neighbors (bonds 12 and 16). The distance between the centers of the rings on which the TE resides is 4.19 Å , in excellent agreement with the distance between the magnetic dipoles obtained from the PLDMR data where $r_{ub}=3.52$ Å . Finally, we note that the conclusion that the TE responsible for the triplet PLDMR is highly localized and of size comparable to one to two phenylene rings is in excellent agreement with the patterns of the localized triplets observed in C_{60} and C_{70} films.[42]

TABLE I. Upper limit of triplet wave function extent r_{ub} in Å determined from light induced electron spin resonance (Ref. 29), from PLDMR (Refs. 12, 46, and 46, this work) or polarizability of the excitations (Ref. 36, for a spherical$^{(a)}$ or cubic$^{(b)}$ shape).

Materials	$D/g\mu_\beta$ (G)	r_{ub} (in Å), $C_1=30.2$	r_{ub} (in Å), $C_2=24.1$
EC2T (Ref. 29)	1041	2.99	2.38
EC3T (Ref. 29)	841	3.21	2.55
EC4T (Ref. 29)	730	3.36	2.68
EC5T (Ref. 29)	690	3.43	2.73
EC5T (Ref. 36)		$3.52^{(a)}$	$2.84^{(b)}$
EC6T (Ref. 29)	670	3.46	2.75
P3HT (Ref. 12)	560	3.67	2.92
P8T (Ref. 36)		$3.63^{(a)}$	$2.92^{(b)}$
PT (Ref. 29)	475	3.88	3.09
PPV (Ref. 46)	521	3.77	3.00
LOPP7 (this work)	705	3.39	2.71
m-LPPP (this work)	620	3.52	2.83
photo-oxidized m-LPPP (this work)	620	3.52	2.83

D. Effects of the localization on the electron phonon coupling.

In the PA spectra of m-LPPP (see Fig. 4) we observe at least two vibrational modes with energies of 80 and 180 meV, which also appear in the absorption and electromodulation spectra.[43] The strength of the different vibronic peaks is determined by the overlap of the wave functions of the electronic ground and excited states, which take their vibronic excitation n_i and n_j' into account. The normal mode vibrational wave functions form an orthonormal set

$$\langle \psi(\nu_i) | \psi(\nu_j') \rangle = \delta_{ij}\delta_{\nu\nu'} . \tag{3}$$

Hence, if the geometries of the ground and excited state of a molecule do not change only the $i=j$ transitions will be allowed, leading to a dominant 0-0 transition.[44] Therefore, the occurrence of a vibronic progression (VP) is a consequence of a change in the equilibrium geometry between the ground and excited states. This change is expressed by the Huang-Rhys parameter, i.e., the change in the linear electron-phonon interaction, which indicates how many phonons are involved in the electronic transitions.

The polaron PA band at ~1.9 eV reveals a VP of 180 meV which is also observed in the absorption and electromodulation spectra of m-LPPP.[43] This 180-meV vibrational mode is well known to be due to the stretching vibration of the C=C-C=C structure of the polymer backbone.

In contrast, the TE PA band exhibits only a weak vibrational mode with an energy of ~80 meV. This mode is also clearly detectable in absorption as well as low-temperature electromodulation spectra.[43] The reason for the absence of the 180 meV mode in this band was revealed by previous

quantum chemical calculations, which derived the geometric relaxation energy between T_1 and T_n in the triplet manifold in trans-stilbene.[45] It was found that the relaxation energy is of the order of 50 meV, which suggests that the potentials of T_1 and T_n are only displaced vertically in a configuration coordinate model. This corresponds to a highly dominant 0-0 transition (low Huang Rhys factor), as discussed above. A low relaxation energy can either correspond to a substantial displacement of a few C atoms upon photoexcitation or a slight displacement of many C atoms. The former case would explain the current experimental PLDMR and PA results as well as the quantum chemical calculations.

The low intensity of the VP is attributed to the relatively high-binding energy of the TE, which may be higher than 1 eV in PPV's.[37] Such a high-binding energy and localization lead to a small change in the geometry upon excitation and therefore to a weak VP in the $T_1 \rightarrow T_n$ absorption and a dominant 0-0 transition, which suggests reduced vibronic activity.

IV. CONCLUSIONS

In conclusion we have shown that photo-oxidation of m-LPPP films increases the intensity of the polaron resonance as well as the polaron PA band at 1.9 eV. This is attributed to increased interchain polaron pair formation due to the increased defect concentration, which is also confirmed by an increased photocurrent in m-LPPP devices. From the analysis of the triplet powder pattern of m-LPPP and LOPP7 and from quantum chemical calculations for an isolated LOPP7 molecule we conclude that the TE wave function is highly localized and of size comparable to one to two phenylene rings. The experimentally determined increase of the wave-function extent from 3.39 Å for LOPP7 to 3.52 Å for m-LPPP is in agreement with the experimental results obtained for other polymers as well as with quantum chemical calculations for isolated molecules. The observation of a weak VP in the $T_1 \rightarrow T_n$ absorption as well as the observation of a 80 meV mode are assigned to the difference in the nature of the localization of the TE wave-function.

ACKNOWLEDGMENTS

The quantum-chemical calculations were carried out during a research stay of E.Z. at the University of Mons-Hainaut. E.Z. is grateful to D. A. dos Santos, D. Beljonne, and J. L. Bredas for valuable discussions. The authors also thank E.L. Frankevich for fruitful discussions. E.J.W.L. gratefully acknowledges the support of the Austrian FWF (Project No. 12806) and of the BMWV. The work in Graz was partially supported by the SFB Elektroaktive Stoffe. E.Z. acknowledges the financial support of the ÖAW. Ames Laboratory is operated by Iowa State University for the U.S. Department of Energy under Contract No. W-7405-Eng-82. This work was supported by the Director for Energy Research, Office of Basic Energy Sciences.

APPENDIX

The spin Hamiltonian H_{ss} has three principal solutions for the magnetic field when its direction coincides with one of the principal axes of the triplet wave-function, which is assumed to be approximately cylindrically symmetric about the z axis.[27,30] These solutions yield the following characteristics of the full-field triplet powder spectrum:

(1) Steps at $H_{1,2} \approx 1/g\mu_\beta (h\nu \pm D)$
(2) Shoulders at $H_{3,4} \approx 1/g\mu_\beta (h\nu \pm (D+3E)/2)$
(3) Singularities at $H_{5,6} \approx 1/g\mu_\beta (h\nu \pm (D-3E)/2)$.

Since by definition of the principal axes $|E| \leqslant |D|/3$, the full-field powder pattern is contained in the range $H_1 \leqslant H \leqslant H_2$.

The minimum, singularities, shoulders, and steps of the half-field powder pattern occur at the following fields

(1) Minimum at $H_{\min} \approx 1/2g\mu_\beta \sqrt{(h\nu)^2 - 4(D^2+3E^2)/3}$
(2) Singularity at $H_{si} \approx 1/2g\mu_\beta \sqrt{(h\nu)^2 - (D+E)^2}$
(3) Shoulder at $H_{sh} \approx 1/2g\mu_\beta \sqrt{(h\nu)^2 - (D-E)^2}$
(4) Step at $H_{\max} \approx 1/2g\mu_\beta \sqrt{(h\nu)^2 - 4E^2}$.

[1] S. Tasch, A. Niko, G. Leising, and U. Scherf, Appl. Phys. Lett. **68**, 1090 (1996).
[2] S. Tasch, G. Kranzelbinder, G. Leising, and U. Scherf, Phys. Rev. B **55**, 1 (1997).
[3] W. Graupner, S. Eder, M. Mauri, G. Leising, and U. Scherf, Synth. Met. **69**, 419 (1995).
[4] M. G. Harrison, S. Müller, G. Weiser, G. Urbasch, R. F. Mahrt, H. Bässler, and U. Scherf, Phys. Rev. B **60**, 8650 (1999).
[5] C. Zenz, W. Graupner, S. Tasch, G. Leising, K. Müllen, and U. Scherf, Appl. Phys. Lett. **71**, 2566 (1997); S. Stagira, M. Zavelani-Rossi, M. Nisoli, S. DeSilvestri, G. Lanzani, C. Zenz, P. Mataloni, and G. Leising, *ibid.* **73**, 2860 (1998); B. Schweitzer, G. Wegmann, D. Hertel, R. F. Mahrt, H. Bassler, F. Uckert, U. Scherf, and K. Müllen, Phys. Rev. B **59**, 4112 (1999).
[6] S. Tasch, E. J. W. List, O. Ekström, W. Graupner, G. Leising, P. Schlichting, U. Rohr, Y. Geerts, U. Scherf, and K. Müllen, Appl. Phys. Lett. **71**, 2883 (1997).
[7] S. Tasch, E. J. W. List, C. Hochfilzer, G. Leising, P. Schlichting, U. Rohr, Y. Geerts, U. Scherf, and K. Müllen, Phys. Rev. B **56**, 4479 (1997).
[8] M. Wohlgenannt, W. Graupner, G. Leising, and Z. Vardeny, Phys. Rev. Lett. **82**, 3344 (1999); Phys. Rev. B **60**, 5321 (1999).
[9] W. Graupner, G. Leising, G. Lanzani, M. Nisoli, S. de Silvestri, and U. Scherf, Phys. Rev. Lett. **76**, 847 (1996); W. Graupner, G. Cerullo, G. Lanzani, M. Nisoli, S. De Silvestri, E. J. W. List, and G. Leising, *ibid.* **81**, 3259 (1998); V. I. Arkhipov, E. V. Emelianova, and H. Bässler, Chem. Phys. Lett. **296**, 452 (1998); B. Schweitzer, V. I. Arkhipov, and H. Bassler, *ibid.* **304**, 365 (1999).
[10] Z. Shuai, D. Beljonne, J. L. Brédas, and R. J. Silbey, Phys. Rev. Lett. **84**, 131 (2000).
[11] Y. Cao, I. D. Parker, G. Yu, C. Zhang, and A. J. Heeger, Nature (London) **397**, 414 (1999).
[12] D. Beljonne, J. Cornil, R. H. Friend, R. A. J. Janssen, and J. L. Brédas, J. Am. Chem. Soc. **118**, 6453 (1996).
[13] L. S. Swanson, J. Shinar, and K. Yoshino, Phys. Rev. Lett. **65**, 1140 (1990).
[14] L. S. Swanson, J. Shinar, A. R. Brown, D. D. C. Bradley, R. H.

Friend, P. L. Burn, A. Kraft, and A. B. Holmes, Phys. Rev. B **46**, 15 072 (1992).
[15] L. S. Swanson, F. Lu, J. Shinar, Y. W. Ding, and T. J. Barton, Proc. SPIE **1910**, 101 (1993). Note that PPE and poly(phenylene acetylene) (PPA) are synonymous.
[16] E. L. Frankevich, A. A. Lymarev, I. Sokolik, F. E. Karasz, S. Blumstengel, R. H. Baughman, and H. H. Hörhold, Phys. Rev. B **46**, 9320 (1992).
[17] E. L. Frankevich, G. E. Zoriniants, A. N. Chaban, M. M. Triebel, S. Blumstengel, and V. M. Kobryanskii, Chem. Phys. Lett. **261**, 545 (1996).
[18] U. Scherf and K. Müllen, Makromol. Chem., Rapid Commun. **12**, 489 (1991).
[19] J. Grimme and U. Scherf, Makromol. Chem. **197**, 2297 (1996).
[20] M. Yan, L. J. Rothberg, F. Papadimitrakopoulos, M. E. Galvin, and T. M. Miller, Phys. Rev. Lett. **73**, 744 (1994).
[21] W. Graupner, M. Sacher, M. Graupner, C. Zenz, G. Grampp, A. Hermetter, and G. Leising, in *Electrical, Optical, and Magnetic Properties of Organic Solid-State Materials IV*, edited by J.R. Reynolds *et al.*, MRS Symposia Proceedings No. 488 (Materials Research Society, Pittsburgh, 1998), p. 789.
[22] L. S. Swanson, J. Shinar, L. R. Lichty, and K. Yoshino, in *Advanced Organic Solid State Materials*, edited by L. Y. Chiang, P. M. Chaikin, and D. O. Cowan, MRS Symposia Proceeding No. 173 (Materials Research Society, Pittsburgh, 1990), p. 385.
[23] W. Graupner, J. Partee, J. Shinar, G. Leising, and U. Scherf, Phys. Rev. Lett. **77**, 2033 (1996).
[24] W. Graupner, T. Jost, K. Petritsch, S. Tasch, G. Leising, M. Graupner, and A. Hermetter, Annu. Tech. Conf.-Soc. Plast. Eng. **XLIII**, 1339 (1997).
[25] G. Feistritzer, Diploma Thesis at TU-Graz, 1999.
[26] W. Graupner, S. Eder, M. Mauri, G. Leising, and U. Scherf, Synth. Met. **69**, 419 (1995).
[27] R. E. Coffman and A. Pezesck, J. Magn. Reson. **70**, 21 (1986).
[28] J. A. Weil, *Electron Paramagnetic Resonance* (Wiley, New York, 1994).
[29] C. P. Poole, *Electron Spin Resonance: a Comprehensive Treatise on Experimental Techniques* (Wiley, New York, 1983).
[30] M. Bennati, A. Grupp, M. Mehring, and P. Bäuerle, J. Phys. Chem. **100**, 2849 (1996).
[31] Z. V. Vardeny, X. Wei, in *Handbook of Conducting Polymers*, 2nd ed., edited by T. A. Skotheim, R. L. Elsenbaumer, and J. Reynolds (Dekker, New York, 1997).
[32] A. Carrington and A. D. McLachlan, *Introduction to Magnetic Resonance* (Harper and Row, New York, 1967); N. M. Atherton, *Electron Spin Resonance* (Halstead, New York, 1973).
[33] P. C. Taylor *et al.*, Chem. Rev. **75**, 203 (1975).
[34] J. Köhler, Phys. Bl., **52**, 669 (1996).
[35] E. J. W. List, J. Partee, W. Graupner, J. Shinar, and G. Leising (unpublished).
[36] E. J. W. List, G. Leising, J. Partee, J. Shinar, U. Scherf, K. Müllen, and W. Graupner (unpublished).
[37] J. M. Warman, G. H. Gelinck, J. J. Piet, J. W. A. Suykerbuyk, M. P. de Haas, B. M. W. Langveld-Voss, R. A. J. Janssen, D. H. Hwang, A. B. Holmes, M. Remmers, D. Neher, K. Müllen, and P. Bäuerle, Proc. SPIE **3145**, 142 (1997).
[38] D. Beljonne, Z. Shuai, R. H. Friend, and J. L. Brédas, J. Chem. Phys. **102**, 2042 (1995).
[39] M. J. S. Dewar, E. G. Zoebisch, E. F. Healy, and J. J. P. Stewart, J. Am. Chem. Soc. **107**, 3902 (1985).
[40] D. A. dos Santos, D. Beljonne, J. Cornil, and J. L. Brédas, Chem. Phys. **227**, 1 (1998).
[41] E. Zojer, J. Cornil, G. Leising, and J. L. Brédas (unpublished).
[42] P. A. Lane and J. Shinar, Phys. Rev. B **51**, 10 028 (1995).
[43] G. Meinhardt, A. Horvath, G. Weiser, G. Leising, and U. Scherf, Synth. Met. **84**, 669 (1997).
[44] J. L. Bredas, J. Cornil, and A. J. Heeger, Adv. Mater. **8**, 447 (1996).
[45] Z. G. Soos, S. Ramasesha, D. S. Galvao, and S. Etemad, Phys. Rev. B **47**, 1742 (1993).
[46] L. S. Swanson, P. A. Lane, J. Shinar, and F. Wudl, Phys. Rev. B **44**, 10 617 (1991).